Journal of Solid State Chemistry 182 (2009) 2555–2559

Contents lists available at ScienceDirect

Journal of Solid State Chemistry

journal homepage: www.elsevier.com/locate/jssc

# Solvent-dependent luminescent Cu(I) framework based on 5-(4-pyridyl)tetrazole

Fei Wang, Rongmin Yu, Qi-Sheng Zhang, Zhen-Guo Zhao, Xiao-Yuan Wu, Yi-Ming Xie, Li Qin, Shan-Ci Chen, Can-Zhong Lu *

*State Key Laboratory of Structural Chemistry, Fujian Institute of Research on the Structure of Matter, Chinese Academy of Sciences, Fuzhou, Fujian 35002, China*

ARTICLE INFO

*Article history:*
Received 6 March 2009
Received in revised form
28 May 2009
Accepted 2 June 2009
Available online 8 July 2009

*Keywords:*
MOF
π–π interaction
Luminescence
Gas absorption

ABSTRACT

A new Cu(I) coordination compound, $Cu_4(L)_4 \cdot 2EtOH$ (**1**), has been obtained from the solvothermal reaction of CuBr, HL (L = 5-(4-pyridyl) tetrazole), EtOH and $NH_3 \cdot H_2O$. The structure determination reveals that **1** has a 2D network, where each Cu(I) atom adopts a trigonal coordination mode. The 2D networks stacked in an ABAB sequence through the π–π interaction to form a 3D supramolecular framework, giving a 1D channel along the *b*-axis. The TGA and powder XRD measurements reveal that the framework is stable after removal of the guest molecules. Gas ($N_2$) adsorption measurement was carried out for the framework. Framework **1** shows II sorption profile with $N_2$, which indicates that $N_2$ molecules cannot diffuse into the micropore and only surface adsorption occurs. The photoluminescent research shows that compound **1** displays an interesting solvent-dependent luminescence.



## 1. Introduction

The rational design of metal-organic frameworks (MOFs) has attracted considerable attention because of their potential applications in catalysis [1], separation [2], ion exchange [3], and gas sorption and storage [4]. The major task of the synthesis for such MOFs is to choose appropriate metal-connecting nodes and/or organic-bridging ligands to control the formation of these complexes with required structures and properties. Long-bridged ligands or large secondary building units have been used to obtain some porous MOFs, while crystal structures with such large cavities are usually stabilized by inclusion of either suitable guests or interpenetrating lattices [5] and the absence of the guest molecules often results in low thermal stability of the host framework. Consequently, the synthesis of robust open frameworks with both high porosity and thermal stability is still a big challenge for chemists. Weak interactions such as hydrogen bonding and π–π interaction are also important in the architecture of porous MOFs [6]. The 5-substituted tetrazole derivatives, with plentiful coordinate ability and possibility, have been used extensively in the synthesis of coordination polymers with interesting structural and/or physical properties, such as luminescence, non-linear optics, ferroelectricity, magnetism and porosity [7–9]. The ligand 5-(4-pyridyl)tetrazole (HL) is an interesting multifunctional ligand having a rich store of N atoms to bind metal ions and to form hydrogen bonds. So far, a few complexes based on pyridyl-substituted tetrazole compounds have been reported in recent years [10]; the coordination chemistry of the HL ligand remains largely unexplored.

Despite the large number of solvent-dependent luminescent materials described in the literature, they are mainly organic molecule materials [11]; reports of solvent-dependent luminescent MOFs are scarce [12]. Herein, we report the synthesis, characterization and properties of HL bridged porous, two-dimensional coordination framework $Cu_4(L)_4 \cdot 2EtOH$ (**1**), which exhibits an interesting solvent-dependent luminescence.

## 2. Experimental

### 2.1. Materials and methods

The HL ligand was synthesized in accordance with the procedure reported by Demko and Sharpless [13]. The IR spectra (KBr pellets) were recorded on a Magna 750 FT-IR spectrophotometer. Powder X-ray diffraction data were recorded on a Rigaku MultiFlex diffractometer with a scan speed of 0.05–0.2° $min^{-1}$. Thermal stability studies were carried out on a NETSCHZ STA-449C thermoanalyzer under $N_2$ (30–800 °C range) at a heating rate of 10 °C $min^{-1}$. Fluorescence spectra were measured with a HORIBA Jobin-Yvon FluoroMax-4 spectrometer equipped with an integrating sphere. The adsorption isotherm of $N_2$ (77 K) was measured in the gaseous state using ASAP-2020 volumetric adsorption equipment.

* Corresponding author. Fax: +86 591 83705794.
*E-mail address:* czlu@fjirsm.ac.cn (C.-Z. Lu).

0022-4596/$ - see front matter © 2009 Elsevier Inc. All rights reserved.
doi:10.1016/j.jssc.2009.06.041

### 2.2. Synthesis of $Cu_4(C_6N_5H_4)_4 \cdot 2EtOH$ (**1**)

In a 23-mL Teflon-lined autoclave, a mixture of CuI (0.5 mmol, 0.095 g), HL (1 mol, 1.470 g), EtOH (10 ml) and $NH_3 \cdot H_2O$ (25%, 2 ml) was stirred for about 10 min and then was heated at 150 °C for 3 days. Yellow block crystals were collected, about 0.046 g (40% yield based on Cu). Using other cuprous halides, such as CuCl, $CuCl_2$, CuBr $CuBr_2$ as metal sources by control the mole ratio of the reactants can also obtain **1.** Anal. Calcd. (%) for $C_{28}H_{28}N_{20}O_2Cu_4$: H: 4.74, C: 36.81, N: 17.18. Found: C 36.12, H 3.06, N 29.98. IR (KBr pellet, $cm^{-1}$): 3444b, 1620 s, 1447, 1435, 1057, 1010, 845 m, 720 s.

### 2.3. Crystal structure determination

X-ray diffraction data were collected on a Rigaku Mercury CCD X-ray diffractometer with graphite monochromated Mo-$K\alpha$ radiation ($\lambda = 0.71073$ Å) using a $\omega$ scan technique. CrystalClear software was used for data reduction and empirical absorption correction. The structure was solved by the direct methods using the Siemens SHELXTL$^{TM}$ Version 5 package of crystallographic software [14]. The difference Fourier maps based on the atomic positions yield all non-hydrogen atoms. The hydrogen atom positions were generated theoretically, allowed to ride on their respective parent atoms and included in the structure factor calculations with assigned isotropic thermal parameters but were not refined. The structure was refined using a full-matrix least-squares refinement on $F^2$. All non-hydrogen atoms were refined anisotropically. The summary of crystallographic data and structure analysis is given in Table 1. The selected bond lengths and bond angles are listed in Table 2.

The hydrogen bonding information is listed in Table 3.

Crystallographic data (excluding structure factors) for the structure reported in this paper have been deposited with the Cambridge Crystallographic Data Centre as supplementary publication no. CCDC: 714391. Copies of the data can be obtained free of charge on application to CCDC, 12 Union Road, Cambridge CB2 1EZ, UK (fax: 44 1223 336 033; e-mail: deposit@ccdc.cam.ac.uk).

**Table 1**
Crystal data and structure refinement details for **1**.

| Empirical formula | C28 H28 Cu4 N20 O2 |
|---|---|
| Formula weight | 930.86 |
| Temperature | 293(2) K |
| Wavelength | 0.71073 Å |
| Crystal system | Triclinic |
| Space group | P−1 |
| *a* | 7.223(3) Å |
| *b* | 15.375(8) Å |
| *c* | 16.003(8) Å |
| $\alpha$ | 95.349(18)° |
| $\beta$ | 96.740(13)° |
| $\gamma$ | 98.175(11)° |
| *V* | 1736.0(14) Å$^3$ |
| *Z* | 2 |
| Calculated density | 1.781 Mg/m$^3$ |
| Crystal size | 0.20 × 0.20 × 0.20 mm |
| Limiting indices | $-7 \le h \le 8$, $-18 \le k \le 18$, $-19 \le l \le 18$ |
| Reflections collected/ unique | 11163/6294 |
| Refinement method | Full-matrix least-squares on $F^2$ |
| *R*(int) | 0.0329 |
| Goodness-of-fit on $F^2$ | 1.033 |
| Final *R* indices [*I* > 2sigma(*I*)] | $R_1 = 0.0525$, $\omega R_2 = 0.1545$ |
| *R* indices (all data) | $R_1 = 0.0700$, $\omega R_2 = 0.1664$ |

$R_1 = (|F_o|-|F_c|)/|F_o|$, $\omega R_2 = [w(F_o^2-F_c^2)/w(F_o^2)^2]^{1/2}$.

**Table 2**
Selected bond lengths (Å) and bond angles (deg) for **1**.

| | | | |
|---|---|---|---|
| Cu(1)–(1)#1 | 1.961 (3) | N(1)#1–Cu(1)–N(15)#2 | 123.79 (15) |
| Cu(1)–N(15)#2 | 1.965 (3) | N(1)#1–Cu(1)–N(19) | 117.77 (15) |
| Cu(1)–N(19) | 1.970 (3) | N(15)#2–Cu(1)–N(19) | 118.44 (14) |
| Cu(2)–N(11) | 1.965 (3) | N(11)–Cu(2)–N(5) | 123.72 (15) |
| Cu(2)–N(5) | 1.972 (3) | N(11)–Cu(2)–N(10) | 118.60 (15) |
| Cu(2)–N(10) | 1.980 (3) | N(5)–Cu(2)–N(10) | 117.68 (15) |
| Cu(3)–N(6)#3 | 1.957 (3) | N(6)#3–Cu(3)–N(20) | 124.23 (15) |
| Cu(3)–N(20) | 1.958 (4) | N(6)#3–Cu(3)–N(14)#2 | 118.06 (15) |
| Cu(3)–N(14)#2 | 1.983 (4) | N(20)–Cu(3)–N(14)#2 | 117.69 (14) |
| Cu(4)–N(9) | 1.955 (4) | N(9)–Cu(4)–N(16) | 124.34 (15) |
| Cu(4)–N(16) | 1.958 (4) | N(9)–Cu(4)–N(4) | 118.07 (15) |
| Cu(4)–N(4) | 1.978 (3) | N(16)–Cu(4)–N(4) | 117.58 (15) |

Symmetry codes: #1 *x*+1, *y*+1, *z*; #2 *x*+2, *y*+1, *z*+1; #3 *x*+1, *y*, *z*+1.

**Table 3**
Geometrical parameters of hydrogen bonds of 1.

| | D–H | H···A | D···A | D–H···A |
|---|---|---|---|---|
| O(1)–H(1B)···N(2) | 0.82 | 2.24 | 3.0183 | 158 |
| O(2)H(2B)···N(17) | 0.82 | 2.54 | 2.9986 | 116 |

## 3. Results and discussion

### 3.1. Description of crystal structure

Single-crystal X-ray analysis reveals that compound **1** crystallizes in the triclinic form with space group P-1. In **1**, each Cu(I) atom adopts a trigonal coordination mode with three nitrogen atoms (see Fig. 1) from two different tetrazole rings and one pyridyl ring [Cu–N 1.955(4)–1.983(4) Å] (see Table 2). The ligands are deprotonated to balance the charges of the whole structure according to chemical and structural information. Each L ligand serves as a $\mu_3$-bridge to link three Cu(I) centers through three nitrogen atoms, leading to a 2D layer structure (Fig. 2a). This sheet contains six-numbered circuits ($Cu_2N_4$) and 32-numbered circuits ($Cu_4N_{12}C_{16}$). The Cu–Cu distances in the $Cu_2N_4$ rings are 3.3608(12) and 3.3628(11) Å. The cavity of each $Cu_4N_{12}C_{16}$ ring is filled with one ethanol molecule. There are O–H···N hydrogen bonding interactions (Table 3) between ethanol molecules and tetrazole ligands. The 2D layer structure of **1** can be rationalized as a ($4.8^2$) topological network (Fig. 2b) when Cu and L are regarded as three-connected nodes [15].

It should be pointed out that the adjacent layers are stacked in an ABAB sequence to form a 3D framework, in which the π–π interactions play an important role. Between the interlayers A and B, the centroid distance between pyridyl ring and tetrazole ring is

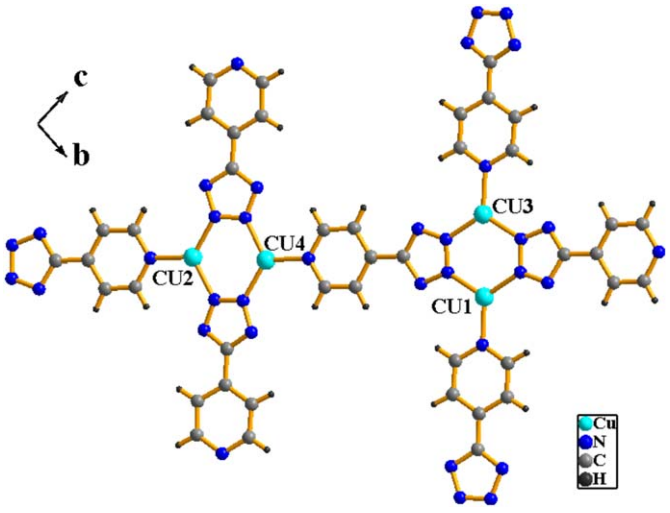


**Fig. 1.** The coordination environment of the Cu atoms.

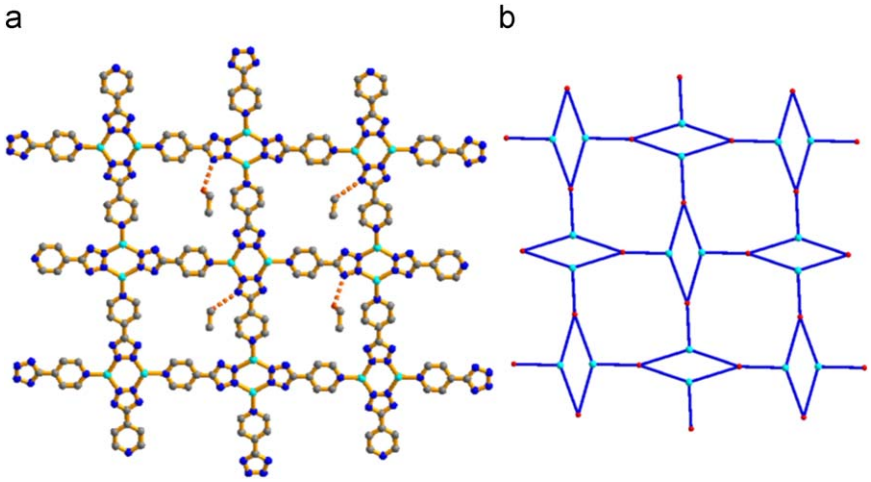


**Fig. 2.** (a) View of the 2D layer structure of **1** parallel to the *b*–*c* plane. (b) 2D three-connected ($4.8^2$) topology network in **1**.

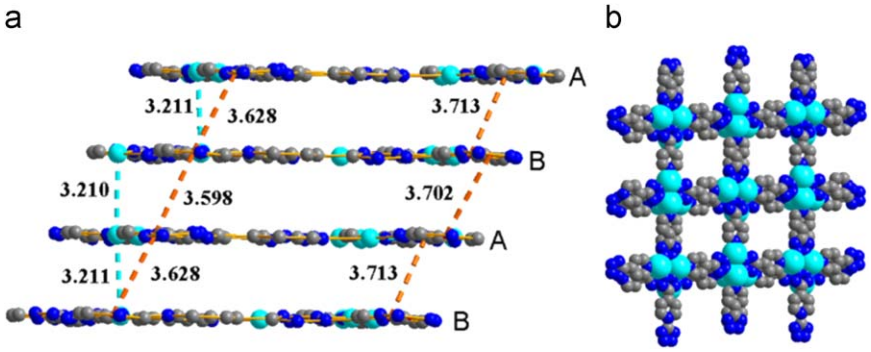


**Fig. 3.** (a) 3D supramolecular framework stacked by π–π interactions indicated by red dashed lines, and inter-$Cu_2$ cuprophilic interactions shown by green dashed lines. Hydrogen atoms and ethanol molecules are omitted for clarity; (b) view of the 3D framework along the *a* axis. For interpretation of the references to color in this figure legend, the reader is referred to the web version of this article.

3.7131(16) Å, the centroid distance between pyridyl rings is 3.6279(16) Å, which are 3.7015(16) and 3.5982(16) Å in the interlayers B and A, respectively (Fig. 3). Besides, together with the π–π interactions, the short Cu–Cu distances [3.211(2) Å for Cu(1)–Cu(4) and 3.210(2) Å for Cu(1)–Cu(2)], which are alternately present in the interlayers, suggest an intermolecular cuprophilic interaction [16], and also help to support the parallel arrangement of the coordination polymer. So the 2D layers are stacked to form a 3D supramolecular framework by the π–π interactions and intermolecular cuprophilic interaction, giving a square channel with pores in dimensions of approximately 6.3 Å × 6.3 Å (Fig. 3b), equal to the length of the ligand.

### 3.2. Thermogravimetric and XRD analysis

To examine thermal stability of these frameworks, thermal gravimetric analysis (TGA) and X-ray powder diffraction patterns (PXRD) measurements were carried out. The TGA curve indicates that a weight loss of 9.37% occurred in the temperature range of 30–85 °C, corresponding to the loss of two guest ethanol molecules (expected 9.40%) and the desolvation form is stable up to about 300 °C and then decomposes to an unidentified product (Fig. 4). To study the framework with the powder XRD technique, samples of **1** were evacuated at 130 °C for 24 h under vacuum, and the XRD patterns of the resultant solid show the main reflections remaining unaltered as the pristine samples of **1**, indicating that the framework structure of **1** is maintained after complete removal of the ethanol molecules (Fig. 5). The solvent

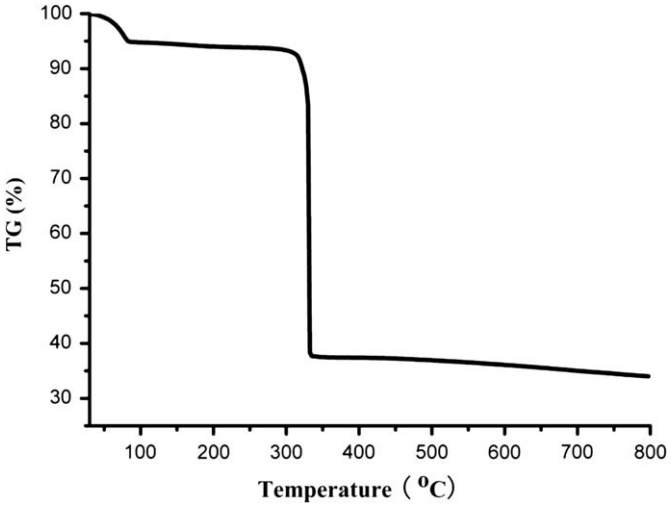


**Fig. 4.** TG curve for **1** under $N_2$ atmosphere.

accessible volume of MOF-1 is estimated by PLATON[11] to be about 24.0% of the total crystal volume.

### 3.3. Gas sorption

We have studied the adsorption property of the framework of **1** with $N_2$. The sorption isotherms of $N_2$ at 77 K of **1** show a II profile

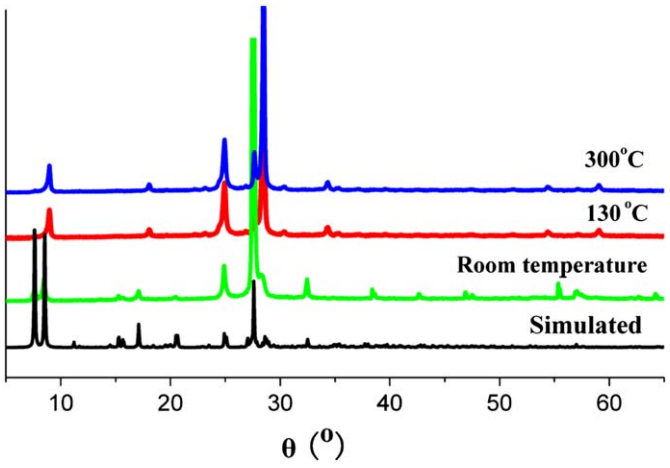


**Fig. 5.** Powder XRD pattern of compound **1**.

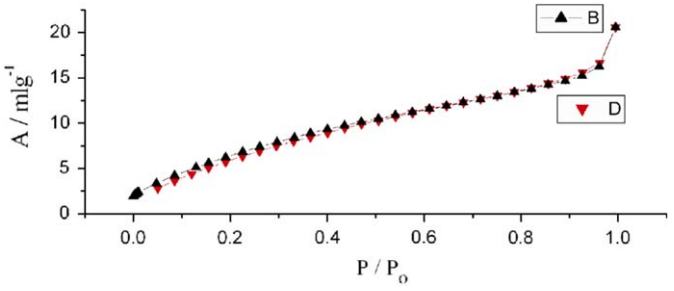


**Fig. 6.** Isotherms for $N_2$ at 77 K: (B) Absorption, (D) Desorption.

(Fig. 6), which indicates that $N_2$ molecules cannot diffuse into the micropore and only surface adsorption occurs. The structure of compound **1** is similar to compound $[Cu(bipy)(1,4\text{-napdc})(H_2O)_2]_n$ [17], and the adsorption property is also similar to it. From this sorption profile, surface area has been determined using the BET equation, which shows 27.32 $m^2 g^{-1}$.

### 3.4. Luminescence property

The photoluminescent property was also investigated in the pure crystals and the desolvation form MOF-1. The as-synthesized crystals appeared transparent yellow and emitted yellow light upon illumination with UV light; with the evaporation of the solvent molecules, the emission disappeared, and the samples were powdered and the color of samples became pale. Interestingly, the emission reappeared when they were soaked in ethanol. The emission peak at about 530 nm upon photoexcitation at 370 nm for compound **1** might be attributed to a metal-to-ligand charge transfer (MLCT) [18]. The pronounced solvatochromism of the fluorescence indicates severe interaction of the fluorescence with the solvent molecules.

The MOF-1 has poor solubility in most organic solvents. To investigate the influence of common organic solvents on the luminescent property of **1**, the effects of eight solvents with different molecular sizes and polarity on the fluorescent emission intensity of **1** were also studied. It was found that the fluorescent intensity of **1** in different solvents followed the order acetone ($Me_2CO$), acetonitrile (MeCN), ethanol (EtOH), methanol (MeOH), ethyl acetate (EtOAc), $CH_2Cl_2$, $CHCl_3$ and hexane, which shows that the fluorescence intensity varies with the polarity of solvents (Fig. 7).

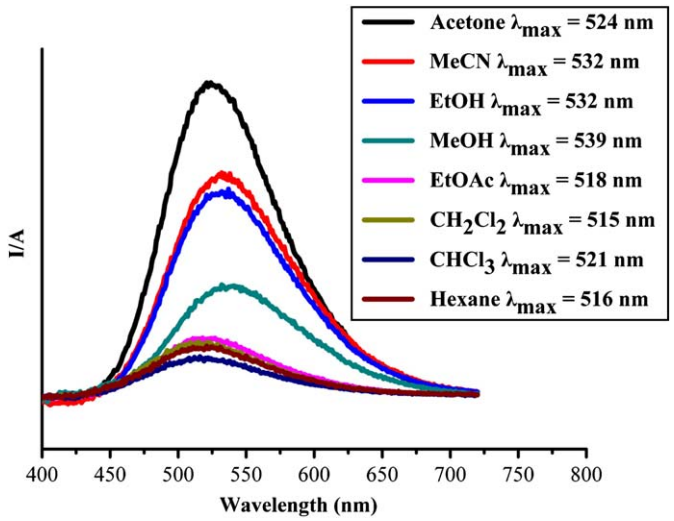


**Fig. 7.** Solid-state fluorescence intensity of **1** in different solvents, showing solvent-dependent fluorescence property of the framework.

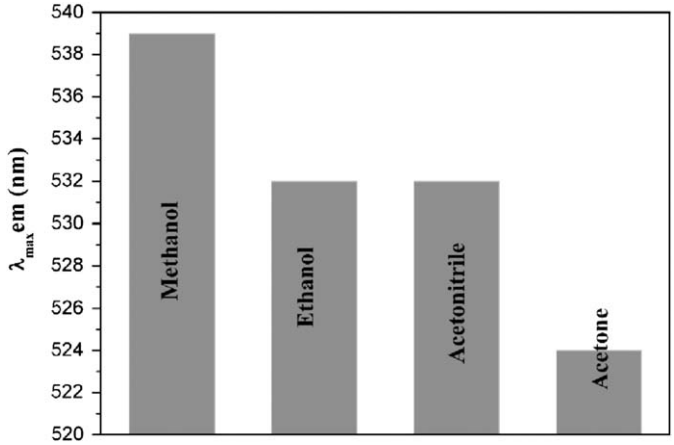


**Fig. 8.** Maximum fluorescence wavelength of MOF-1 in the strong polarity solvents.

The solvent-dependent fluorescence properties of the framework can be attributed to the following aspects: effect of solvent polarity and the interactions between the framework and the guest molecules whether diffuse into the channels or not. As shown in Fig. 7, although weak fluorescence emission peaks were also observed in the weak polar solvents, such as EtOAc, $CH_2Cl_2$, $CHCl_3$ and hexane, the emission intensity of the powder samples of **1** has little change. In the case of strong polar solvents, such as MeOH, EtOH, MeCN, $Me_2CO$, the results have shown that the maximum fluorescence wavelengths in the four solvents were red-shifted when the polarity of solvents solution was increased (Fig. 8) [19].

In addition, guest molecules with large sizes, whose diffusion may be constrained by the channel, would show no or only a weak effect on the fluorescence property of the framework. As mentioned above, there exists a 1D channel in MOF-1. Methanol, MeCN, being smaller than EtOH, can diffuse into channels of the framework more than EtOH and show strong influence of MOF-1. The weak interaction may exist between the guest solvent molecules and the Cu center, which adopts the trigonal coordination mode; meanwhile, MeOH and EtOH can also interact with the L ligands by O–H···N interactions. So the intensity and the maximum emission wavelength are more affected in MeOH than

in others. The intensity is strongest and red-shifted of the maximum emission wavelength is least in $Me_2CO$, mainly due to the coordination ability of the acetone molecule being less compared to MeCN, MeOH and EtOH, while the size of the $Me_2CO$ molecules is large compared to MeCN, MeOH and EtOH [17]. The result shows that solvent polarity and the interactions between the framework and the solvent molecules should play important roles in the solvent-dependent fluorescence behavior of MOF-1.

## 4. Conclusion

In conclusion, we have presented the synthesis, structure, characterization, gas sorption property and photoluminescent property of the new 3D supramolecular MOF. Framework 1 has a 2D rectangular grid network and is stacked in an ABAB sequence to form the 3D framework, which shows an interesting solvent-dependent luminescence. TGA and XRD studies confirm that the porous framework of 1 exhibits high stability against the removal of the guest molecules with thermal conditions. The title compound may be a potential candidate as a photoactive material owing to its fluorescence, thermal stability and insolubility in common polar and non-polar solvents.

## Acknowledgments

This work was supported by the 973 key program of the MOST (2006CB932904, 2007CB815304), the National Natural Science Foundation of China (20425313, 20521101 and 50772113), Chinese Academy of Sciences (KJCX2-YW-M05) and the Natural Science Foundation of Fujian Province (2006L2005).

## References

[1] [a] J.S. Seo, S.I. Jun, K. Kim, Nature 404 (2000) 982–986;
[b] L. Pan, H.-M. Liu, X.-G. Lei, J. Li, Angew. Chem. Int. Ed. 42 (2003) 542–546.
[2] K. Uemura, S. Kitagawa, M. Kondo, Chem. Eur. J. 8 (2002) 3586–3600.
[3] [a] O.M. Yaghi, H.-L. Li, J. Am. Chem. Soc. 117 (1995) 10401–10402;
[b] A. Kamiyama, T. Kajiwara, Angew. Chem. Int. Ed. 39 (2000) 3130–3132.
[4] [a] S. Noro, S. Kitagawa, M. Kondo, Angew. Chem. Int. Ed. 39 (2000) 2081–2084;
[b] M. Eddaoudi, J. Kim, M. O'Keeffe, O.M. Yaghi, Science 295 (2002) 469–472;
[c] N.L. Rosi, J. Eckert, M. O'Keeffe, O.M. Yaghi, Science 300 (2003) 1127–1129;
[d] D.N. Dybtsev, H. Chun, K. Kim, J. Am. Chem. Soc. 126 (2004) 32–33;
[e] L. Pan, M.B. Sander, J. Li, J. Am. Chem. Soc. 126 (2004) 1308–1309.
[5] K. Biradha, M. Fujita, Angew. Chem. Int. Ed. 41 (2002) 3395–3398.
[6] D. Li, K. Kaneko, Chem. Phys. Lett. 335 (2001) 50–56.
[7] [a] J.-R. Li, Y. Tao, Q. Yu, X.-H. Bu, Chem. Commun. (2007) 1527–1529;
[b] J. Tao, Z.-J. Ma, R.-B. Huang, Inorg. Chem. 43 (2004) 6133–6135;
[c] H. Deng, Y.-C. Qiu, Y.-H. Li, R.-H. Zeng, Chem. Commun. (2008) 2239–2241.
[8] [a] R.-G. Xiong, X. Xue, X.-Z. You, Angew. Chem. Int. Ed. 41 (2002) 3800–3803;
[b] X.-S. Wang, Y.-Z. Tang, R.-G. Xiong, Inorg. Chem. 44 (2005) 5278–5285;
[c] Q. Ye, Y.-H. Li, Huang, R.-G. Xiong, Inorg. Chem. 44 (2005) 3618–3625;
[d] Q. Ye, Y.-Z. Tang, R.-G. Xiong, Dalton Trans. (2005) 1570–1573;
[e] Q. Ye, Y.-M. Song, R.-G. Xiong, J. Am. Chem. Soc. 128 (2006) 6554–6555;
[f] H. Zhao, Z.-R. Qu, R.-G. Xiong, Chem. Soc. Rev. 37 (2008) 84–100.
[9] [a] A. Rodríguez, R. Kivekäs, E. Colacio, Chem.Commun. (2005) 5228–5230;
[b] M. Dincă, A.F. Yu, J.R. Long, J. Am. Chem. Soc. 128 (2006) 8904–8913;
[c] M. Dincă, W.S. Han, J.R. Long, Angew. Chem. Int. Ed. 46 (2007) 1419–1422;
[d] Y. Zou, S. Hong, M.S. Lah, Chem. Commun. (2007) 5182–5184.
[10] [a] F.A. Mautner, C. Gspan, K. Gatterer, Polyhedron 23 (2004) 1217–1224;
[b] P. Lin, W. Clegg, R.A. Henderson, Dalton Trans. (2005) 2388–2394;
[c] C. Jiang, Z.-P. Yu, Y. Cui, Eur. J. Inorg. Chem. (2004) 3662–3667;
[d] X. Xue, X.-S. Wang, R.-G. Xiong, Inorg. Chem. 41 (2002) 6544–6546;
[e] X.-S. Wang, R.-G. Xiong, Chin. J. Inorg. Chem. 21 (2005) 1025–1029;
[f] S. Bhandari, C.G. Frost, Dalton Trans. (2000) 663–669.
[11] [a] W.-W. Qin, T. Rohand, M. Baruah, A. Stefan, Chem. Phys. Lett. 420 (2006) 562–568;
[b] M. Baruah, W.-W. Qin, C. Flors, J. Phys. Chem. A 110 (2006) 5998–6009;
[c] N. Armaroli, G. Marconi, L. Echegoyen, Chem. Eur. J. 6 (2000) 1629–1645;
[d] H. Detert, E. Sugiono, G. Kruse, J. Phys. Org. Chem. 15 (2002) 638–641;
[e] A. Sarkar, S. Chakravorti, J. Lumin. 78 (1998) 205–211;
[f] D.E. Bergbreiter, H.N. Gray, B. Srinivas, Macromolecules 27 (1994) 7294–7301.
[12] [a] Y. Bai, G.J. He, C.Y. Duan, Q.J. Meng, Chem. Commun. (2006) 1530–1532;
[b] L.-G. Qiu, Z.-Q. Li, Y. Wu, W. Wang, Chem. Commun. (2008) 3642–3644.
[13] Z.P. Demko, K.B. Sharpless, J. Org. Chem. 66 (2001) 7945–7950.
[14] [a] Rigaku (2002), CrystalClear Version 1.35, Rigaku Corporation.; Siemens (1994), SAINT Software Reference Manual, Siemens Energy & Automation Inc., Madison, WI, USA.;
[b] Siemens (1994), SHELXTLTM Version 5 Reference Manual, Siemens Energy & Automation Inc., Madison, WI, USA.
[15] [a] T. Wu, R. Zhou, D. Li, Inorg. Chem. Commun. 9 (2006) 341–345;
[b] Q.-G. Zhai, X.-Y. Wu, C.-Z. Lu, Cryst. Growth Des. 6 (2006) 2126–2135.
[16] J.-X. Zhang, J. He, D. Li, Inorg. Chem. 47 (2008) 3471–3473.
[17] T.K. Maji, M. Ohba, S. Kitagawa, Inorg. Chem. 44 (2005) 9225–9231.
[18] X.-H. Huang, T.-L. Sheng, X.-T. Wu, Inorg. Chem. Commun. 9 (2006) 1304–1307.
[19] [a] O. Crauβ, U. Lommatzsch, C. Lahmann, Phys. Chem. Chem. Phys. 3 (2001) 74–79;
[b] S.-B. Park, J.S. Suh, K.-W. Lee, J. Ind. Eng. Chem. 8 (2002) 46–49.